# *Supplementary Materials*
# Modeling of a Thick Cylindrical Pneumatic Leg for a Soft Parallel Robot

Zeinab Awada[1], Hamza El Jjouaui[1], Marc Gouttefarde[1], Yassine Haddab[1]
[1]LIRMM, Univ Montpellier, CNRS, Montpellier, France.

This article serves as supplementary material to the conference paper entitled "Modeling of a Thick Cylindrical Pneumatic Leg for a Soft Parallel Robot" submitted to 2024 IEEE International Conference on Soft Robotics (RoboSoft). The equations and figures are numbered in accordance with the main paper and the same symbols are used.

Using the Yeoh model to present the strain energy density function, the analytical solutions of the pressure and the external axial force are presented in Section 1 and Section 2, respectively. The sensitivity analysis of the pressure and the axial force models with respect to the Yeoh material constants is given in Section 3. Finally, the experimental aspect is confronted in Section 4. Four identical thick cylindrical actuators are fabricated and pressurized progressively to check the impact of the used material on the performance of the actuator.

## Contents

# 1 Pressure Model Analytical Expression

Using the Yeoh material model [2], the strain energy density function, $W$, is expressed as follows

$$W = \sum_{i=1}^{N} C_i \left(\lambda_r^2 + \lambda_\theta^2 + \lambda_z^2 - 3\right)^i \tag{27}$$

$N$ is the polynomial order of the model, $C_i$ is the material constant, and $\lambda_r$, $\lambda_\theta$, and $\lambda_z$ are the radial, azimuth, and axial stretches respectively.
Given that $\lambda_{in}$ is the radial stretch at the internal wall of the cylinder, $\lambda_{ex}$ is the radial stretch at the external wall of the cylinder, and $\lambda_z$ is the axial stretch, the pressure model reads

$$\Delta p = \tilde{p}(\lambda_{in}, \lambda_z) - \tilde{p}(\lambda_{ex}, \lambda_z) \tag{28}$$

where $\tilde{p}(\lambda_\theta, \lambda_z)$ is

$$\begin{aligned}
\tilde{p}(\lambda_\theta, \lambda_z) = {} & \frac{-6C_3\lambda_z - C_1 + 6C_2 - 27C_3 - 2C_2\lambda_z^{-1} + 18C_3\lambda_z^{-1}}{\lambda_z^2\lambda_\theta^2} \\
& + \frac{-6C_3\lambda_\theta^2 - 3C_3\lambda_z^2 - 2C_2 + 9C_3 - 1.5C_3\lambda_z^{-1} - C_3\lambda_z^{-2}\lambda_\theta^{-2}}{\lambda_z^4\lambda_\theta^4} \\
& + \frac{-1.5C_3\lambda_\theta^4\lambda_z + 3C_3\lambda_\theta^2}{\lambda_z^2} + \frac{\lambda_\theta^2\left(2C_2 - 18C_3\right)}{\lambda_z} + \frac{12C_3\ln\lambda_\theta}{\lambda_z^3} \\
& + \frac{-3C_3\lambda_z^2 + 6C_3\lambda_\theta^4\lambda_z + 18C_3 - 2C_2}{\lambda_\theta^2} \\
& + \frac{\ln\lambda_\theta\left(2C_1 - 12C_2 + 54C_3 + 4C_2\lambda_z^{-1} - 36C_3\lambda_z^{-1}\right)}{\lambda_z} \\
& + \lambda_z\ln\lambda_\theta\left(4C_2 - 36C_3 + 6C_3\lambda_z^2 + 12C_3\lambda_z^{-1}\right)
\end{aligned}$$

## 2 Force Model Analytical Expression

The external axial force model $f_{ex}$ reads

$$f_{ex} = \tilde{f}(\lambda_{in}, \lambda_z) - \tilde{f}(\lambda_{ex}, \lambda_z) \tag{29}$$

where $\tilde{f}(\lambda_\theta, \lambda_z)$ is

$$\begin{aligned}
\tilde{f}(\lambda_\theta, \lambda_z) =& (\pi(\lambda_z\lambda_{in}^2 - 1))(6C_3\lambda_\theta^2 - 12\ln(\lambda_\theta^2\lambda_z - 1)\frac{C_2}{\lambda_z^2} + 54\ln(\lambda_\theta^2\lambda_z - 1)\frac{C_3}{\lambda_z^2} + 8\ln(\lambda_\theta^2\lambda_z - 1)\frac{C_2}{\lambda_z^3} \\
&- 72\ln(\lambda_\theta^2\lambda_z - 1)\frac{C_3}{\lambda_z^3} + 24\ln(\lambda_\theta^2\lambda_z - 1)\frac{C_3}{\lambda_z^4} - 4C_1\ln(\lambda_\theta)\frac{1}{\lambda_z^2} + 24C_2\ln(\lambda_\theta)\frac{1}{\lambda_z^2} + \frac{3C_3}{\lambda_z^6\lambda_\theta^4} \\
&+ 2\ln(\lambda_\theta^2\lambda_z - 1)\frac{C_1}{\lambda_z^2} - 16C_2\ln(\lambda_\theta)\frac{1}{\lambda_z^3} + 144C_3\ln(\lambda_\theta)\frac{1}{\lambda_z^3} - 60C_3\ln(\lambda_\theta)\frac{1}{\lambda_z^4} + \frac{12C_3}{\lambda_z^5\lambda_\theta^2} \\
&+ \frac{2C_1}{\lambda_z^2(\lambda_\theta^2\lambda_z - 1)} - \frac{12C_2}{\lambda_z^2(\lambda_\theta^2\lambda_z - 1)} + \frac{8C_2}{\lambda_z^3(\lambda_\theta^2\lambda_z - 1)} + \frac{24C_3}{\lambda_z^4(\lambda_\theta^2\lambda_z - 1)} + \frac{4C_2}{\lambda_z^4\lambda_\theta^2} - \frac{36C_3}{\lambda_z^4\lambda_\theta^2} \\
&- 24\ln(\lambda_\theta)\frac{C_3}{\lambda_z} - 108\ln(\lambda_\theta)\frac{C_3}{\lambda_z^2} + \frac{54C_3}{\lambda_z^2(\lambda_\theta^2\lambda_z - 1)} - \frac{72C_3}{\lambda_z^3(\lambda_\theta^2\lambda_z - 1)} + \frac{6C_3}{\lambda_z^2\lambda_\theta^2} \\
&- \frac{2\lambda_z C_1}{\lambda_\theta^2\lambda_z - 1} + \frac{12\lambda_z C_2}{\lambda_\theta^2\lambda_z - 1} - \frac{54\lambda_z C_3}{\lambda_\theta^2\lambda_z - 1} - 4\frac{C_2}{\lambda_\theta^2\lambda_z - 1} + 36\frac{C_3}{\lambda_\theta^2\lambda_z - 1} + 4\ln(\lambda_\theta^2\lambda_z - 1)C_2 \\
&- 36\ln(\lambda_\theta^2\lambda_z - 1)C_3 + 24C_3\ln(\lambda_\theta^2\lambda_z - 1)\frac{1}{\lambda_z} - \frac{6\lambda_z^5 C_3}{\lambda_\theta^2\lambda_z - 1} + 12C_3\ln(\lambda_\theta)\lambda_z^2 - \frac{4\lambda_z^3 C_2}{\lambda_\theta^2\lambda_z - 1} \\
&+ \frac{36\lambda_z^3 C_3}{\lambda_\theta^2\lambda_z - 1} - \frac{18\lambda_z^2 C_3}{\lambda_\theta^2\lambda_z - 1} + 6C_3\ln(\lambda_\theta^2\lambda_z - 1)\lambda_z^2 - 6C_3\lambda_\theta^2 - 2C_2\lambda_\theta^2\frac{1}{\lambda_z^2} + 18C_3\lambda_\theta^2\frac{1}{\lambda_z^2} \\
&- \frac{3}{2}C_3\lambda_\theta^4\frac{1}{\lambda_z^2} - 6C_3\lambda_\theta^2\frac{1}{\lambda_z^3} + 12\ln(\lambda_\theta^2\lambda_z - 1)\frac{C_2}{\lambda_z^2} - 54\ln(\lambda_\theta^2\lambda_z - 1)\frac{C_3}{\lambda_z^2} - 8\ln(\lambda_\theta^2\lambda_z - 1)\frac{C_2}{\lambda_z^3} \\
&+ 72\ln(\lambda_\theta^2\lambda_z - 1)C_3\frac{1}{\lambda_z^3} - 24\ln(\lambda_\theta^2\lambda_z - 1)C_3\frac{1}{\lambda_z^4} - 2C_1\ln(\lambda_\theta)\frac{1}{\lambda_z^2} - 12C_2\ln(\lambda_\theta)\frac{1}{\lambda_z^2} \\
&- 2\ln(\lambda_\theta^2\lambda_z - 1)C_1\frac{1}{\lambda_z^2} + 8C_2\ln(\lambda_\theta)\frac{1}{\lambda_z^3} - 72C_3\ln(\lambda_\theta)\frac{1}{\lambda_z^3} + 24C_3\ln(\lambda_\theta)\frac{1}{\lambda_z^4} - \frac{3}{2}C_3\frac{1}{\lambda_z^6\lambda_\theta^4} \\
&- \frac{6C_3}{\lambda_z^5\lambda_\theta^2} - \frac{2C_2}{\lambda_z^4\lambda_\theta^2} + \frac{18C_3}{\lambda_z^4\lambda_\theta^2} + 24\ln(\lambda_\theta)C_3\frac{1}{\lambda_z} + 54\ln(\lambda_\theta)C_3\frac{1}{\lambda_z^2} + 4C_2\ln(\lambda_\theta) \\
&- \frac{6C_3}{\lambda_z^2\lambda_\theta^2} - 36\ln(\lambda_\theta^2\lambda_z - 1)C_3 - 4\ln(\lambda_\theta^2\lambda_z - 1)C_2 + 36\ln(\lambda_\theta^2\lambda_z - 1)C_3 - 6C_3\ln(\lambda_\theta^2\lambda_z - 1)\lambda_z^2 \\
&- 24\frac{C_3}{\lambda_z}\ln(\lambda_\theta^2\lambda_z - 1) + 6C_3\ln(\lambda_\theta)\lambda_z^2)
\end{aligned}$$

# 3 Pressure and Force Model Sensitivity to Material Constants

As mentioned in the main article, the sensitivity analysis of the pressure and the axial force models as a function of the three Yeoh material constants ($C_1$, $C_2$, and $C_3$) is studied. For this purpose, these constants are varied by ± 30% with respect to the chosen reference model of Ecoflex™ 0050- Smooth-on Inc., $C_{1r} = 15.8$, $C_{2r} = 0.48$, and $C_{3r} = 0.113$ kPa [1]. The results are reported in Fig. 10. This study yields the following findings: (1) The maximum variations in the pressure and force models $\varepsilon_{max}$ show a linear correlation with the alterations in $C_1$, $C_2$, and $C_3$. (2) Among the three material constants, $C_2$ has a minimal impact, yet it equally affects $\Delta p$ and $f_{ex}$. A 30% change in $C_2$ results in a 5% variation in both models. (3) $C_1$ exerts the most significant influence on $\Delta p$ for low ranges of deformation. A 30% change in $C_1$ causes a 30% variation in $\Delta p$ and a 21.6% variation in $f_{ex}$. (4) Inversely, $C_3$ has the most influence on $f_{ex}$ for high ranges of deformation. A 30% change in $C_3$ causes about 24% variations in both $f_{ex}$ and $\Delta p$. (5) Finally, $\varepsilon_{max}$ is always symmetric with respect to the y-axis. For example, a -10% decrease and a +10% increase in any of the material constants yield the same $\varepsilon_{max}$.

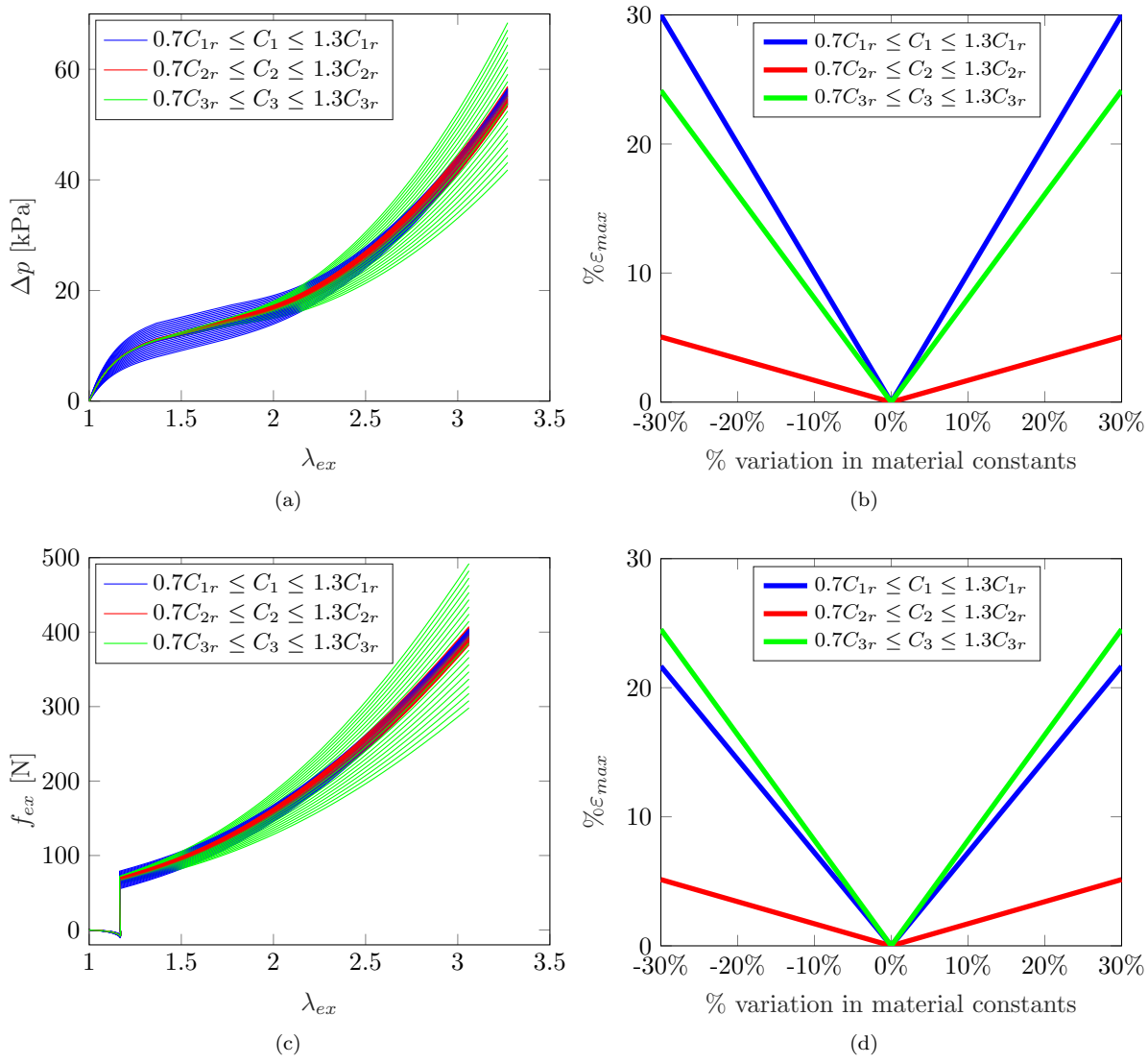


Figure 10: (a) $\Delta p$ and (c) $f_{ex}$ versus the external radial deformation $\lambda_{ex}$ and the corresponding maximum variations $\varepsilon_{max}$ (b) and (d) repectively, when the three Yeoh material constants are altered by ± 30% with respect to the reference values: $C_{1r} = 15.8$, $C_{2r} = 0.48$, and $C_{3r} = 0.113$ kPa. $\varepsilon_{max}$ is calculated with respect to a reference $\Delta p$ and $f_{ex}$ corresponding to the reference material constants $C_{1r}$, $C_{2r}$, and $C_{3r}$.

# 4 Experimental Results of Different Samples

The previous section demonstrates the importance of the material used and its characterization on the pressure and force models. It is therefore pertinent to test how the impact of the material translates in experiments.

For this purpose, four thick cylindrical actuators are fabricated using molding. Two different boxes of Ecoflex™ 0050, Smooth-on Inc. from different sources are used and two samples are prepared from each box. These boxes have been subjected to different storing conditions that we have no trace of. Therefore, fabricating actuators from two different boxes serves an indicator of how variable external factors, e.g. temperature, might influence the material and hence the performance of the cylindrical actuator. Moreover, two actuators are fabricated from the same box to augment the dataset though within the constraints of a limited sample size.

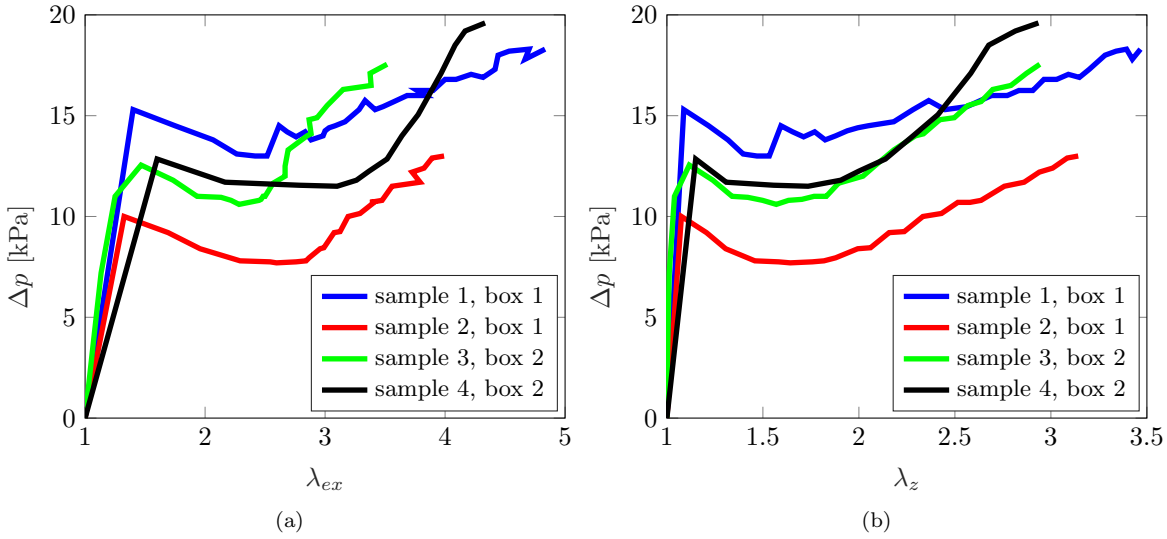


Figure 11: $\Delta p$ versus (a) $\lambda_{ex}$ and (b) $\lambda_z$ for four different samples of a thick cylindrical actuator.

The four actuators are progressively pressurized and the consequent $\Delta p$ versus the external radial stretch $\lambda_{ex}$ and the axial stretch $\lambda_z$ are plotted in Fig. 11. Roughly speaking, Fig. 11(b) shows that the plots for $\Delta p$ of samples 1, 2, and 3 follow the same tendency. However, a considerable shift is noticed between them. For example, knowing that the maximum recorded pressure for the second sample (red curve) is 13 kPa, an almost constant difference of about 5 kPa with the first sample (blue curve) can be seen over the range of deformation of the actuator. Moreover, the performance of the second sample (red curve) and the third (green curve) is very similar with an average pressure difference of 3 kPa for ($\lambda_{ex} \leq 2.5$, $\lambda_z \leq 2$). Beyond this state of deformation, the average difference in pressure between the two samples increases to 6 kPa and 4.7 kPa in the $\Delta p$ - $\lambda_{ex}$ and $\Delta p$ - $\lambda_z$ planes respectively. As for samples 3 (green curve) and 4 (black curve) both of which are fabricated from the same box, considering the $\Delta p$ - $\lambda_z$ plane, the percentage difference in $\Delta p$ is limited to 9% for $\lambda_z \leq$ 2.4. It then increases to 11.7% for higher ranges of deformation. However in the $\Delta p$ - $\lambda_{ex}$ plane, the two samples are significantly different with a difference of 40% for $\lambda_{ex} = 3$ for example.

We therefore notice that the first two samples fabricated from the same box, have a similar behavior despite an almost constant difference of 5 kPa for a given state of deformation $(\lambda_{ex}, \lambda_z)$. On the other hand, the behavior of samples 3 and 4 are quite different especially in the $\Delta p$ - $\lambda_{ex}$ plane. The number of samples does not allow a conclusive decision if whether or not sample four is an outlier and hence considering that the other three actuators have a similar behavior with a constant difference in the pressure value for a given state of deformation. In conclusion, given the high non-linearity of the actuator and the several bifurcation phenomena associated to it [3, 4], it is challenging to narrow the reasons for the variable performances reported in Fig. 11. However, using the same molds for fabrication, it remains clear that the storing conditions are to be highly considered when preparing the actuators and characterizing the material used.

# References


[1] D. Sarkar, S. Chakraborty, A. Arora, and S. Sen, "A Reinforced Soft Bending-type Actuator with Improved Performance and Force Sensing: Design, Analysis and Experiments," in *Advances in Robotics - 5th International Conference of The Robotics Society.* Kanpur India: ACM, Jun. 2021, pp. 1–6.

[2] O. H. Yeoh, "Some forms of the strain energy function for rubber," *Rubber Chemistry and technology*, vol. 66, pp. 745–771, Nov. 1993.

[3] D. M. Taghizadeh, A. Bagheri, and H. Darijani, "On the Hyperelastic Pressurized Thick-Walled Spherical Shells and Cylindrical Tubes Using the Analytical Closed-Form Solutions," *International Journal of Applied Mechanics*, vol. 07, no. 02, p. 1550027, Apr. 2015.

[4] D. Haughton and R. Ogden, "Bifurcation of inflated circular cylinders of elastic material under axial loading—II. Exact theory for thickwalled tubes," Journal of the Mechanics and Physics of Solids, vol. 27, no. 5-6, pp. 489–512, Dec. 1979.